Published in final edited form as:
Microvasc Res. 2015 March ; 98: 108–118. doi:10.1016/j.mvr.2015.01.008.

Regulation of valve endothelial cell vasculogenic network architectures with ROCK and Rac inhibitors

C. Alexander Arevalos, **Amanda T. Walborn**, **Amanda A. Rupert**, **Jonathan M. Berg**, **Elizabeth L. Godfrey**, **Jacqueline M.V. Nguyen**, and **K. Jane Grande-Allen**
Department of Bioengineering, Rice University, Houston, TX, USA

Abstract

Objective—The age- and disease-dependent presence of microvessels within heart valves is an understudied characteristic of these tissues. Neovascularization involves endothelial cell (EC) migration and cytoskeletal reorientation, which are heavily regulated by the Rho family of GTPases. Given that valve ECs demonstrate unique mesenchymal transdifferentiation and cytoskeletal mechanoresponsiveness, compared to vascular ECs, this study quantified the effect of inhibiting two members of the Rho family on vasculogenic network formation by valve ECs.

Approach and results—A tubule-like structure vasculogenesis assay (assessing lacunarity, junction density, and vessel density) was performed with porcine aortic valve ECs treated with small molecule inhibitors of Rho-associated serine-threonine protein kinase (ROCK), Y-27632, or the Rac1 inhibitor, NSC-23766. Actin coordination, cell number, and cell migration were assessed through immunocytochemistry, MTT assay, and scratch wound healing assay. ROCK inhibition reduced network lacunarity and interrupted proper cell–cell adhesion and actin coordination. Rac1 inhibition increased lacunarity and delayed actin-mediated network formation. ROCK inhibition alone significantly inhibited migration, whereas both ROCK and Rac1 inhibition significantly reduced cell number over time compared to controls. Compared to a vascular EC line, the valve ECs generated a network with larger total vessel length, but a less smooth appearance.

Conclusions—Both ROCK and Rac1 inhibition interfered with key processes in vascular network formation by valve ECs. This is the first report of manipulation of valve EC vasculogenic organization in response to small molecule inhibitors. Further study is warranted to comprehend this facet of valvular cell biology and pathology and how it differs from vascular biology.

Keywords

Aortic valve; Valve endothelial cell; Vasculogenesis; Rho kinase; Rac1

Introduction

Calcific aortic valve disease (CAVD) has a prevalence of about 3% in patients older than 75 and leads to ~ 50,000 heart valve replacements each year (Go et al., 2014). Neovascularization (the formation of new blood vessels) is a well-recognized histological

Disclosures
The authors have nothing to disclose.

characteristic of CAVD (Chalajour et al., 2004a, Chalajour et al., 2007, Charest et al., 2006, Hakuno et al., 2010, Mariscalco et al., 2011, Mazzone et al., 2004, Paranya et al., 2001, Poggio et al., 2011, Rajamannan et al., 2005, Soini et al., 2003 and Syväranta et al., 2010). Angiogenesis, the process in which new vessels and capillaries sprout from existing ones, is also known to promote mineralization within diverse tissues, thereby contributing to the progressive hardening and resultant lack of function in pathologies such as atherosclerosis or ectopic bone formation (Collett and Canfield, 2005). The cell-mediated mechanisms of angiogenesis have not been widely investigated in CAVD, with some notable exceptions. The glycoprotein chondromodulin, which is anti-angiogenic, was demonstrated to be abundant in normal adult heart valves but present in lower amounts in regions of diseased heart valves marked by neovascularization (Yoshioka et al., 2006).

It has been proposed that a targeted antiangiogenic therapy could stop the progression of valve disease by preventing the entrance of excess nutrients and inflammatory infiltrates through neovessels generated by the valve endothelial cells (VECs) (Hakuno et al., 2010). Statin-based, lipid-lowering therapies used in the treatment of atherosclerosis progression do not appear to reduce CAVD progression (Teo et al., 2011). Studies showing that CAVD involves endochondral bone formation (Xu et al., 2010) – a process that, in normal bone, requires neovascularization (Ishijima et al., 2012) – also supports investigating the inhibition of functional neovessel formation as a treatment for CAVD. Interestingly, normal pediatric heart valves (unlike normal adult valves) are richly vascularized (Duran and Gunning, 1968), which suggests that vascularization may be an important factor to consider in the tissue engineering of heart valves for pediatric patients. All in all, there is compelling evidence for further characterization of vasculogenic behavior by heart valve cells.

During angiogenesis, the Rho family of GTPases transduces proangiogenic signals into organized cytoskeletal movements. These GTPases, RhoA, Rac1, and Cdc42, are activated by downstream signaling cascades of the membrane receptors of several angiogenic molecules (Huber et al., 2003). Rac1 regulates lamellipodia formation through activation of p21-activated kinase (PAK), whereas RhoA is involved in cell adhesion and forward movement through regulation of stress fiber formation and contraction via the Rho-associated serine-threonine protein kinase (ROCK), which leads to the phosphorylation of myosin light chain (pMLC) (Defilippi et al., 1999, Huber et al., 2003 and Pollard and Borisy, 2003). Therefore, these proteins transduce angiogenic stimuli into coordinated cellular motility and network formation. Several studies have demonstrated the unique attributes of valve endothelial cells (VECs) compared to vascular-derived endothelial cells (ECs) including their transduction of angiogenic stimuli. Additional sources of differences include the valve cells' physiological predisposition toward endothelial to mesenchymal transdifferentiation during valvulogenesis and their distinct mechanical environment (Butcher et al., 2006, Hinton and Yutzey, 2011, Poggio et al., 2011, Xu et al., 2009, Xu et al., 2010 and Yang et al., 2008). Further, key differences between ECs and VECs arise in the expression of genes and proteins that regulate blood vessel development, angiogenesis, adhesion, migration, and cell fate in in vitro comparisons (Butcher et al., 2004 and Butcher et al., 2006).

Compared to ECs, however, the Rho family of GTPases has had limited study in the context of heart valves. ROCK inhibition was previously shown to block calcific nodule formation by valvular interstitial cells (VICs) (Gu and Masters, 2011) and to inhibit mesenchymal invasion by cultured atrioventricular endocardial cells, which are embryonic precursors to VECs (Sakabe et al., 2006). It was also reported that flow-dependent VEC orientation was independent of PI3K, a downstream effector of Rac1, despite its known role in regulating vascular endothelial cell organization in response to flow and during angiogenesis (Butcher et al., 2004 and Holmes et al., 2007). Given the importance of ROCK and Rac1 in regulating endothelial cell motility and organization during angiogenesis (Hoang et al., 2004), as well as the atypical nature of VEC responses to various angiogenic stimuli (Xu et al., 2009 and Yang et al., 2008), and the potential impact of a VEC-specific anti-angiogenic therapy for the treatment of CAVD (Hakuno et al., 2010), there is compelling motivation for further study of the effects of ROCK and Rac1 inhibition on vasculogenic network formation by heart valve cells.

This study investigated the ability to tune the complex vasculogenic networks using small molecule inhibitors of the ROCK (Y-27632) and Rac (NSC-23766) pathways of adult porcine aortic valve endothelial cells (APAVECs) on Matrigel, a reconstituted basement membrane substrate that has been widely used previously to invoke a vasculogenic response from endothelial cells (Arnaoutova and Kleinman, 2010). Several basement membrane components such as SPARC (Charest et al., 2006), laminin (Afek et al., 1999), and collagen type 4 (Afek et al., 1999), as well as transforming growth factor β (Nakajima et al., 1997) have been found to be increased in fibro-calcific valves compared to normal valves. Thus, Matrigel was used to mimic the transition from an anti-angiogenic to a pro-angiogenic environment that the aortic valve cells experience during the progression of CAVD. The geometry of the resulting vasculogenic networks was controlled using small molecule inhibitors for the ROCK (Y-27632) and Rac1 (NSC-23766) pathways. Since cell migration and proliferation play crucial roles in angiogenesis, the effect of the inhibitors on these outcomes was also assessed. Furthermore, the cells in these networks were immunostained for actin, CD31, and α-smooth muscle actin (α-SMA) to demonstrate how cell phenotypes were affected by ROCK and Rac1 inhibition.

Materials and methods

Isolation, purification, and culture of VECs

Adult porcine aortic valve endothelial cells (APAVECs) were used to model physiologically healthy adult human valve cells due to the established similarities between human and porcine valve physiology (Stephens et al., 2011). Previous studies with human cells have demonstrated that VECs from diseased valves are more angiogenic than those harvested from control tissues (Chalajour et al., 2004a). This study aimed to induce previously healthy, quiescent VECs to enter into the proangiogenic phenotype that is associated with CAVD, and to control this phenotype using small molecule inhibitors. Therefore, all APAVECs were harvested from aortic valve leaflets removed from healthy 6-month old pig hearts received from a local abattoir (Fisher Ham and Meats, Houston, TX).

VECs were harvested using a protocol modified from previously described techniques (Butcher et al., 2004 and Cheung et al., 2008). Multiple cell harvests were performed to ensure biological replication, and in each harvest, VECs were pooled from the aortic valve leaflets of 3 separate hearts. In brief, valve leaflets were soaked in an enzyme digest composed of 2 U/mL of dispase (Stemcell, Tukwila, WA) and 60 U/mL of collagenase type II (Worthington Biochemical, Lakewood, NJ) and horizontally shaken at 37 °C for 1 h. After the enzyme digestion, the VECs were lifted from the leaflet by gently rolling a sterile cotton swab over the entire surface. The cells were removed from the cotton swab with multiple washes of EBM-2 media (Lonza, Basel, Switzerland) containing 1% penicillin/streptomycin solution (Lonza) and the growth factor bullet kit EGM-2 (Lonza), which includes epidermal growth factor, hydrocortisone, gentamicin, amphotericin-B, vascular endothelial growth factor (VEGF), fibroblast growth factor beta, R3-insulin like growth factor 1, ascorbic acid, heparin, and fetal bovine serum. The cell suspension was then plated onto sterile 2.5% gelatin-coated T-75 tissue culture flasks and cultured in a humidified incubator at 37 °C and 5% CO2. After reaching confluence, the valve cells were gently removed from the flask using Trypsin EDTA 1 × (Corning, Manassas, MA) and magnetically sorted for CD31 to ensure VEC purity using the Dynabeads Pan Mouse IgG kit (Invitrogen, Carlsbad, CA). Resulting VEC populations were cultured in EBM-2 media at 37 °C and 5% CO2 in preparation for use in subsequent experiments. An immortalized murine cardiac endothelial cell line (MCEC, CELLutions Biosystems, Ontario, Canada) was commercially acquired and cultured in the same manner as the VECs (He et al., 2008).

Tubule-like structure (TLS) vasculogenesis assay

The TLS assay is widely used to study vasculogenesis in cultured cells (Arnaoutova and Kleinman, 2010). This study investigated the extent to which APAVECs cultured from healthy aortic valves could form complex vasculogenic networks on Matrigel, a reconstituted basement membrane substrate that has been widely used previously to invoke a vasculogenic response from endothelial cells (Arnaoutova and Kleinman, 2010). The geometry of the resulting networks was altered using small molecule inhibitors for ROCK and Rac1.

Prior to the start of each study, phenol red free Matrigel (BD Biosciences, San Jose, CA) was thawed overnight on ice. On day 1, 50 μl volumes of cold Matrigel were added to the wells of a 96-well plate and then placed in the incubator at 37 °C for 1 h to allow for gelation. APAVECs in EGM-2 (100 μl) were then plated on top of the Matrigel at a concentration of 24,000 cells per well. In each assay in this study, controls and treatment groups were pipetted from the same source of mixed cells to ensure the same number of cells was seeded each time. Upon seeding, the cells were treated with the ROCK inhibitor Y-27632 (Sigma-Aldrich Research Biochemicals Inc., St. Louis, MO) or the Rac1 inhibitor NSC-23766 (Tocris Bioscience, Bristol, UK) at the concentrations noted below. Controls were treated with PBS. Plates were then returned to the incubator. After 7 h, the resultant tubule-like network structures were imaged in the middle of each well using phase contrast microscopy with a 10 × objective. Each condition was applied to at least triplicate wells, and the assay was repeated three separate times.

For a comparison of baseline vasculogenic network formation between the valvular and vascular cells, the MCECs were cultured under the same TLS assay conditions, but were not subjected to ROCK or Rac1 inhibition.

Automated image analysis for tubule characterization

Phase contrast microscopy can be utilized to image vessel formation in a high throughput manner without interrupting the vessel formation, but this approach suffers from a lack of contrast when imaging cells grown on gels. To circumvent this limitation and allow for downstream analysis, a custom automated script written for ImageJ (Bethesda, MD) was used to convert the phase contrast images to a binary mask using an edge detection algorithm that ignores small and circular objects, allowing it to only detect elongated tubule networks. All images obtained during the TLS experiments were processed using this script prior to quantification of network parameters.

Quantitative analysis of vascular networks is not standardized across labs or fields. Most commonly this work proceeds in a non-automated fashion that is a labor intensive process and prone to human error and biases. The free, open source software Angiotool (Zudaire et al., 2011) offers an automated mechanism to quantify several angiogenesis network metrics in a high throughput and repeatable manner. In brief, the binary images generated from the ImageJ script were convolved with a fast reclusive Gaussian kernel, and the tube-like structures were then computed based on the combination of the eigenvalues of the 2D Hessian matrix. The vessel response was computed for a set of scales that denotes the standard width of the Gaussian filter, and was then in turn interpreted as vessel diameter in the graphical user interface. These features were then skeletonized and analyzed for several angiogenesis metrics: number of junctions, junction density, vessel length, number of endpoints, and average lacunarity. Lacunarity is a parameter that describes the distribution of the sizes of gaps surrounding an object within an image. Greater lacunarity reflects a greater size distribution of these gaps and lower lacunarity reflects a more uniform size distribution. Lacunarity can be used to distinguish objects with similar fractal dimensions, and can be used in general for describing the spatial pattern in which neovascularization occurs (Gould et al., 2011). Supplemental Figure 1 shows representative images of skeletonized networks treated with Y-27632 and NSC-23766.

Immunocytochemistry

In order to image the tubule-like network structures to assess the coordination of cell–cell interactions and actin throughout the networks, the TLS assay was repeated in an 8-well #1 glass chamber slides (Thermo Fisher, Waltham, MA) and immunocytochemistry was performed on the resultant networks to elucidate the localization of CD31, alpha smooth muscle actin (aSMA), and F-actin after 7 h. A volume of 218 μl of Matrigel was added to each well of an 8-well #1 glass chamber slides (Thermo Fisher, Waltham, MA) and allowed to harden as previously described for the TLS assay. In order to maintain the same seeding density of cells as in previous studies, 52,000 APAVECs in 218 μl of EGM-2 media were added to each well and incubated with either the ROCK inhibitor (50 μM) or the Rac1 inhibitor (100 μM) for 7 h at 37 °C. PBS was added in the control condition. The resultant tubule-like structure networks were fixed using 4% paraformaldehyde for 30 min at room

temperature. The cells were then washed with PBS followed by treatment with 0.1% Triton X-100 for 5 min to permeabilize the cell membranes. A blocking solution of 10% donkey serum (Jackson ImmunoResearch, West Grove, PA) and 2% bovine serum albumin (Sigma-Aldrich, St. Louis, MO) was then applied for 1 h at room temperature. Cells were washed again with PBS prior to an overnight incubation with primary antibodies for CD31 (ab28364, 1:100, Abcam, Cambridge, UK) and aSMA (ab7817, 1:100, Abcam) diluted in the blocking solution at 4 °C. Following exposure to primary antibodies, cells were washed with PBS and incubated with the fluorescent secondary antibodies AlexaFluor 555 (A-31572, 1:200, Invitrogen) and AlexaFluor 633 (A-21052, 1:200, Invitrogen) in the same blocking agent overnight at 4 °C. The cells were then stained with phalloidin 488 (A12379, 1:200, Invitrogen) for 20 min. After a final wash with PBS, fluoromount containing DAPI (to demonstrate the cell nuclei) was applied to each well. The networks were then imaged using a confocal fluorescence microscope (Zeiss LSM Live 5, Oberkochen, Germany) using 10 × and 20 × objectives. The images were evaluated to assess the APAVECS' expression of CD31 to confirm their endothelial phenotype, their expression of aSMA to ascertain whether transdifferentiation had occurred, and their overall cell–cell and actin cytoskeleton organization using phalloidin 488. Live-Dead staining was performed by adding 1 μM of calcein-AM (Sigma-Aldrich Research Biochemicals Inc.) and 2 μM of ethidium bromide (Sigma-Aldrich Research Biochemicals Inc.) to the Matrigel-seeded cells 7 h after treatment with ROCK or Rac inhibitors. Thirty minutes later, cells were then washed with PBS and imaged using confocal fluorescence microscopy.

MTT assay for cell number

An assay for MTT (3-(4,5-dimethylthiazol-2-yl)-2,5-diphenyltetrazolium bromide; Sigma-Aldrich, St. Louis, MO, USA) was performed to quantify relative changes in number of APAVECs due to ROCK and Rac1 inhibition (Takada et al., 2004). In brief, 120,000 APAVECs were seeded on a gelatin-coated 24-well plate and incubated at 37 °C for 24 h with the ROCK inhibitor Y-27632 (10, 50, or 100 μM) or the Rac1 inhibitor NSC-23766 (20, 100, or 200 μM). The final concentrations of these inhibitors were selected to range from 5-fold below the EC50 to 2-fold above the EC50 (Ishizaki et al., 2000 and Lee et al., 2007); this range captured the upper range of the concentrations used for the TLS assay. The control group received only PBS. The media was then replaced with 500 μl of 1% BGS and 100 μl of MTT reagent (5 mg/ml sterile MTT in PBS) for 4 h at 37 °C. 1 ml of MTT solvent (DMSO) was then added to each well and triturated thoroughly. The resultant absorbance was read (570 nm–670 nm) using a spectrophotometer (SpectraMax M2; Molecular Devices, Sunnyvale, CA, USA). Six independent wells were tested per treatment group.

Cell migration assay

To observe the migratory behaviors of cells in the presence on ROCK and Rac1 inhibitors, APAVECs were first seeded on gelatin-coated 48-well plates and allowed to grow to confluence in a volume of 200 μl of medium. A cross-shaped wound was then made in the cell layer of each well using a vertical and horizontal scratch from a sterile 200 μl pipette tip. The media was changed and a 3 μl aliquot of the ROCK inhibitor Y-27632 or the Rac1 inhibitor NSC-23766 was added was added to achieve the same range of concentrations as described above for the MTT assay. In the control group, cells received a treatment of only

PBS. In a negative control group, media was instead replaced with EGM2 containing neither serum nor bullet kit. An image was taken at the intersection of the vertical and horizontal scratches using a 10 × objective with phase contrast microscopy at hour 0. After 24 h, another image was taken at the same location in each well. Percent wound healing was quantified as previously reported (Rodriguez et al., 2005) and reported normalized to the control treated with PBS. This study was performed with a total n = 4–6 for each condition.

Statistical analysis

A one-way ANOVA was performed followed by a Tukey HSD for post hoc analysis to analyze for differences between groups in all assays. Statistical significance was accepted for $p < 0.05$.

Results

APAVECs formed tubule-like-structures (TLS) in an angiogenic environment

Since the source of the cells responsible for the neovascularization in the aortic valves during CAVD has not been definitively determined (Chalajour et al., 2004b), we sought to establish the ability of CD31-positive APAVECs to form vasculogenic networks and to quantify the complexity of any networks formed. After 7 h, the CD31+ APAVECs formed a pronounced vascular network structure with readily quantifiable vessel density, junction density, total number of junctions, total number of end points, total vessel length, and lacunarity (Table 1).

ROCK inhibition increased network complexity in a dose dependent manner

As ROCK is an important mediator of angiogenesis, APAVECs were treated with a logarithmic range of concentrations of the ROCK inhibitor Y-27632. At 1, 10, and 100 μM of Y-27632, the resulting APAVEC networks displayed significantly increased vessel density, junction density, and total network length compared to the untreated control networks ($p < 0.0001$, Fig. 1). At these same concentrations, the number of junctions, vessel percentage area, and total number of end points were increased (193, 260, and 290%; 130, 144, and 144%; and 93, 134, and 158%, respectively; data not shown). There was also a significant decrease in lacunarity of the network structures with increased concentrations of Y-27632 ($p < 0.005$, Fig. 1).

Rac1 inhibition decreased network complexity and inhibits network initiation

As shown in Fig. 2, APAVECs treated with the highest dose of 200 μM of the Rac1 inhibitor NSC-23766 displayed significantly decreased total numbers of junctions ($p < 0.01$) and vessel percentage area ($p < 0.01$), and the treatment increased lacunarity ($p < 0.05$) compared to the control. Whereas ROCK inhibition dose-dependently changed the geometry of the vasculogenic networks as indicated by the average lacunarity and junction density, the highest concentration of Rac1 inhibition actually blocked the formation of vasculogenic networks. Although Rac1 inhibition (at 200 μM) decreased the total number of junctions, it did not decrease the overall degree of branching, since there was no change in junction density (data not shown). Furthermore, the network metrics in the groups treated with Rac1 inhibitor did not display dose dependency to the same extent as the ROCK inhibitor.

Although differences in the network morphology could be observed at Rac1 inhibitor concentrations of 2 and 20 μM as shown by Figs. 2A–C, these differences were not statistically significant. The dramatic changes in the network metrics at the higher concentration, however, could be attributed in part to the inability of the software to quantify the lack of a network.

ROCK and Rac1 inhibition influenced cell assemblies

Immunostaining analysis of the APAVEC vasculogenic networks demonstrated that the cells maintained their endothelial phenotype in each condition as demonstrated by positive staining for CD31 (Fig. 3, green). Since alpha smooth muscle actin (αSMA) positive cells that co-express endothelial markers have been shown to sprout from calcific aortic valves (Chalajour et al., 2007), αSMA expression in APAVEC vasculogenic network formation was also assessed. In each sample, a small number of αSMA+/CD31− cells were found along the exterior borders of the tubule structures as shown in Fig. 4A. As demonstrated by the actin stain and CD31 localization, the control samples demonstrated tightly assembled, multicellular, linear tubule-like structures as shown in Fig. 3 and Fig. 4. Structures formed in the presence of Rac1 inhibitor displayed a similar multicellular tube-like morphology, but overall these tube-like structures were fewer in number compared to the control (Fig. 3C). As shown in Fig. 3B, the ROCK-inhibited cells formed multicellular networks, but displayed more flattened junctions and extensions, as opposed to the tube-like morphology characteristics of the control.

The higher magnification images allowed for improved visualization of cell–cell organization through the localization of the homologous cell–cell binding protein CD31. Both the control and Rac1-inhibited multicellular structures displayed tightly organized cell assemblies, whereas ROCK inhibition appeared to interrupt this organization during vasculogenic network formation, resulting in a looser cell assembly (Fig. 4B). A small number of αSMA+ VECs were apparent in each condition as shown by Fig. 4A. In each of these cases, these cells appeared to be co-localizing and binding several CD31+/αSMA− VECs at the same time.

Changes in the network assemblies was not due to cell death, as demonstrated by the lack of ethidium bromide staining and ubiquitous presence of positive calcein AM staining in the Live/Dead assay as shown in Supplemental Figure 2, and by the dynamic motion of the cells as shown in Supplemental Figure 3.

Rac and ROCK inhibition significantly decreased APAVEC number

One of the more dramatic events of angiogenesis is a sudden and rapid increase in endothelial cell proliferation (Kalluri, 2003). The resulting normalized change in MTT absorbance, as a measure of cell number, is shown in Fig. 5. The number of APAVECs was significantly reduced by both Rac (reduced by 25% at 100 μM and 42% at 200 μM) and ROCK (reduced by 23% at 50 μM and 20% at 100 μM) compared to untreated controls, although Rac1 displayed a greater dose dependency in its effect. No significant effect was found at the lowest doses for either Rac1 or ROCK inhibition.

ROCK inhibition significantly decreased APAVEC migration

Since cell migration is an important process in angiogenesis and valvulogenesis, the effects of ROCK and Rac1 inhibition on APAVEC migration were investigated using a scratch wound healing assay. A comparison of the average wound closure given treatment with the ROCK or Rac inhibitor is shown in Fig. 6. Inhibition of the ROCK pathway with Y-27632 significantly inhibited migration (by 18–19% at the two highest inhibitor concentrations), a finding that is consistent with prior studies that inhibited ROCK in VECs from embryonic aortic valve explants (Sakabe et al., 2006). Inhibition of the Rac pathway with NSC-23766 showed a trend of reducing APAVEC migration at 200 μM (by 26%), but this result was not quite statistically significant ($p = 0.08$). No significant effect was found at the lower inhibitor concentrations.

APAVECs display unique network formation compared to vascular endothelial cells

MCECs were directly compared to APAVECs to elucidate differences in the vasculogenic networks formed by each cell type under baseline conditions. At 7 h, both VECs and MCECs displayed complex branching networks, but the MCEC networks displayed smoother tubule formation as individual cells were more difficult to discern (Fig. 7A). Quantification of the MCEC networks relative to the APAVEC networks demonstrated a 27% larger total network size and 22% lower number of end points for the APAVECs (Fig. 7B). The networks demonstrated no significant difference in lacunarity or junction density between the vascular and valvular cells, but there was a strong trend of the APAVECs having a 15% larger vessel percentage area ($p = 0.07$) and 36% greater total number of junctions ($p = 0.06$).

Discussion

The members of the Rho family of GTPases are important mediators of vascular endothelial cell–cell and actin reorganization during angiogenesis (Hoang et al., 2004). This study investigated the effects of ROCK and Rac1 inhibition on APAVEC reorganization. ROCK was shown to have a role in APAVEC migration and network organization, whereas Rac1 influenced APAVEC proliferation and network initiation. This data provides motivation for further investigation into the targeting of Rho family GTPases for the treatment of CAVD by preventing valve cell reorganization into a vasculogenic network. In addition, it elucidated differences between vascular and valvular endothelial networks.

These ROCK inhibition findings confirmed previously reported effects on VEC migration, and provided new information about the effects of ROCK on vascular network formation by VECs. There has been only limited study regarding the ROCK inhibition of VECs despite its important role in cellular organization (Hoang et al., 2004). Previously, ROCK inhibition was shown to prevent transwell migration by transdifferentiating VECs (Sakabe et al., 2006), as reported here for CD31+ APAVECs using the scratch wound healing assay. As a complement to the migration data, quantifying the changes in the complexity of network formation offers a novel assessment of APAVEC responses to vasculogenic stimuli. These results demonstrated that ROCK inhibition can be utilized to control the geometry of the vascular networks formed by APAVECs. Although ROCK inhibition dose-dependently

increased the number of junctions, the resulting quality of the overall network after ROCK inhibition appeared poor as shown by the flattened nature of the tube-like structures and loosely connected nature of the cell assemblies (arrow in Fig. 4B). This observation is consistent with previous reports demonstrating the role of Rho signaling in pinocytosis-mediated lumen formation, which requires tight cell–cell connections, a tube-like morphology (Davis and Bayless, 2003) and overall vascular endothelial cell organization during angiogenesis (Hoang et al., 2004). The poor network formation found in this TLS assay may be due in part to the ability of the ROCK inhibitor to block cell migration. Rho-ROCK machinery is normally engaged to arrange the cells into tubule structures (Bryan et al., 2010), but when the ROCK pathway is inhibited, the cells are less able to pull themselves to a new location (Lamalice et al., 2007). The resulting cell phenotype resembles that of tip cells, which have spiny, elongated lamellipodia reaching out to their next location (De Smet et al., 2009). Due to the density of the seeded cells, the APAVECs appeared to extend out to one another and form a flattened network with a low average lacunarity with ablated tubule formation.

In contrast to ROCK, the effect of Rac1 inhibition on network formation by APAVECs was less pronounced, except at the highest concentrations, at which few network structures formed. Rac1 is understudied in the field of heart valves, despite its well-known role in the initiation of cellular extensions and lamellipodia, which is a critical step in migration and thus important for angiogenesis (Eming and Hubbell, 2011). The findings of decreased number of junctions, decreased vessel percentage area, and increased lacunarity in APAVECs treated with Rac1 inhibitor are similar to previous reports of decreased network connections in human umbilical vein endothelial cells treated with drugs that inhibit Rac and Cdc42 (Bijman et al., 2006). The smaller APAVEC networks might also be explained by the dose-dependent reduction in cell number for APAVECs treated with NSC-23766, given that cell proliferation is an important facet of tubule elongation during angiogenesis (De Smet et al., 2009). Live/Dead staining of the resultant APAVEC networks at the higher concentration of NSC-23766 displayed no signs of cell death during the timeframe of these experiments (Supplemental Figure 2), therefore the ablated network formation cannot be attributed to cell death but is instead due to an inability of the cells to respond to the Matrigel environment. Rac1 inhibition appeared to affect the initiation of the tubule-like structures, however, the tube-like structures that did form demonstrated tightly clustered assemblies of cells and aligned actin structures, similar to the control tubule-like structures.

Further understanding of the differences between vascular and valvular biology will be crucial to developing targeted valve therapies that minimize systemic side effects. Several studies have demonstrated the unique attributes of VECs compared to vascular-derived endothelial cells (Butcher et al., 2004, Butcher et al., 2006, Hinton and Yutzey, 2011, Poggio et al., 2011, Xu et al., 2009, Xu et al., 2010 and Yang et al., 2008) and this study identified a new set of functional differences between the two. Both cell types formed complex networks, but in this work the VECs formed networks that were visibly and measurably different, and appeared to branch more. Since VEC networks were also demonstrated to be tunable by regulating ROCK and Rac, the regulation of the Rho family of GTPases may play a significant role in the functional differences between vascular and valvular endothelial

cells. Furthermore, modification to that regulation could influence their switch to a more angiogenic phenotype, such as occurs during CAVD.

Taken together, these data, showing that APAVECs can form vasculogenic structures in vitro in a manner that can be regulated by inhibition of ROCK and Rac1, provide compelling motivation for future research investigating this inhibition as an interventional treatment for CAVD. Based upon the network macrostructures from Fig. 1 and Fig. 2, the microstructure changes displayed in Fig. 3 and Fig. 4, and the effects of ROCK and Rac inhibition demonstrated previously in vivo (Bryan et al., 2010, Colomba et al., 2011 and Yin et al., 2007), it is hypothesized that ROCK or Rac inhibition would prevent the functional formation of VEC angiogenic structures in vivo. By manipulating these aspects of cell behavior to block the vascular network architecture, the presumed function of these vessels – delivery of inflammatory infiltrates to VICs and enabling mineralization – could be inhibited to prevent progression to CAVD and stenosis. As angiogenesis is reported to occur more in early to mid-stage calcification (Soini et al., 2003), this treatment could be applied as soon as CAVD is detected using echocardiography. In general, translation of many of the currently investigated pathways (Butcher et al., 2011, Caira et al., 2006, Jian et al., 2003, Mohler et al., 1999, Mohler et al., 2001 and O'Brien et al., 1995) toward interventional treatments for CAVD will likely require the delineation of key characteristics of valvular cells in order to target the valve properly; this body of information, however, is continually expanding (Tao et al., 2012). For example, there is growing interest in how the VECs interact with VICs (Balaoing et al., 2014, Butcher and Nerem, 2006, Gould et al., 2014, Tseng et al., 2014, Wang et al., 2013 and Yoshioka et al., 2006), which could reveal whether the VICs play a role in vasculogenic behavior by the VECs. Furthermore, there are a myriad of biomaterial platforms that have been developed to investigate valvular cell biology and pathology (Benton et al., 2009, Chen et al., 2013, Duan et al., 2013a, Duan et al., 2013b, Durst et al., 2011, Eslami et al., 2014, Gould and Anseth, 2013 and Kirschner et al., 2014); the use of more complex biomimetic in vitro models and in vivo models should facilitate discovery of the conditions that regulate vasculogenesis within heart valves.

As a better understanding of angiogenesis within heart valves is developed, there is also the potential to apply this research to produce improved pediatric tissue engineered heart valves (Weind et al., 2002) and gain further insight into valve developmental pathways. Heart valves in the young normally have a rich microvasculature (Duran and Gunning, 1968). It may be that in young tissue engineered valves, spatio-temporal control of angiogenesis would encourage rapid host integration allowing the tissue to grow with the patient. It has also been proposed that certain aspects of valve disease progression involve triggering dormant developmental pathways (Tao et al., 2012), thus a greater understanding of the many angiogenic mechanisms occurring during valvulogenesis would provide new avenues for the investigation of angiogenesis in CAVD.

There were some limitations to this study. First, although both Y-27632 and NSC-23766 are widely characterized specific inhibitors of the ROCK and Rac1 pathways, the degree of inhibition of these pathways was not quantified by a Rho GTP activation assay. Rather, the range of concentrations of the inhibitors used in this study was based on prior reports and encompassed the IC 50 of both inhibitors (Ishizaki et al., 2000 and Lee et al., 2007).

Differences between the effective concentration ranges of the ROCK and Rac1 inhibitors could be attributed to the availability of their respective targets and their individual strengths, which was not investigated in this study. Second, there are limitations associated with the use of Matrigel. Matrigel is a widely used model for vasculogenesis and angiogenesis, although it may not represent the exact pathological microenvironment experienced by valve cells during the progression of CAVD. Nonetheless, the use of Matrigel is consistent with the reports of increased abundance of selected basement membrane constituents in valve leaflets from CAVD (Afek et al., 1999 and Charest et al., 2006). Thus, the Matrigel was meant to serve as a pro-vasculogenic environment in comparison to the more quiescent gelatin coated environment on which the cells were originally cultured. This change from an anti- to pro-angiogenic environment within diseased heart valves has been well-assessed histologically (Chalajour et al., 2004a, Chalajour et al., 2007, Charest et al., 2006, Hakuno et al., 2010, Mariscalco et al., 2011, Mazzone et al., 2004, Paranya et al., 2001, Poggio et al., 2011, Rajamannan et al., 2005, Soini et al., 2003 and Syväranta et al., 2010). Third, it is possible that the aSMA+ cells in the TLS assay could have arisen from spontaneous transdifferentiation from normal culture conditions. However, there was no immunostaining or morphological evidence for the presence of aSMA+ cells prior to performing the TLS assay.

Conclusion

In this study, we demonstrated the ability of valve endothelial cells to form vasculogenic networks in vitro, which were significantly different from the networks generated by a vascular endothelial cell line, and showed the ability to manipulate the geometry of the resulting vascular networks using ROCK and Rac1 inhibitors. Applying analytical tools for quantifying networks allowed for a novel assessment of the biological response of valve endothelial cells to the vasculogenic environment of Matrigel and the Rho GTPase family inhibitors. The results provide motivation for future research to manipulate this pathway and regulate vasculogenesis within heart valves as needed, either to prevent pathologic mineralization, to promote the formation of a vascular network within pediatric tissue engineered heart valves, or to improve understanding of this fundamental aspect of valvular biology.

Supplementary Material

Refer to Web version on PubMed Central for supplementary material.

Acknowledgments

Sources of funding

This work was funded by American Heart Association grant 11IRG5550052 and a National Science Foundation Graduate Research Fellowship (C.A.A.).

The authors thank Melissa McHale, Ph.D., for editorial assistance and Cindy Farach-Carson, Ph.D., for use of her microscopy equipment.

Abbreviations

APAVECs	adult porcine aortic valve endothelial cells
αSMA	alpha smooth muscle actin
CAVD	calcific aortic valve disease
PAK	p21-activated kinase
pMLC	phosphorylation of myosin light chain
ROCK	Rho-associated serine-threonine protein kinase
TLS	tubule-like structure
VEC	valve endothelial cells
VIC	valvular interstitial cells

References

Afek A, Shoenfeld Y, Manor R, Goldberg I, Ziporen L, George J, Polak-Charcon S, Amigo MC, Garcia-Torres R, Segal R, Kopolovic J. Increased endothelial cell expression of alpha3beta1 integrin in cardiac valvulopathy in the primary (Hughes) and secondary antiphospholipid syndrome. Lupus. 1999; 8:502–507. [PubMed: 10483026]

Arnaoutova I, Kleinman HK. In vitro angiogenesis: endothelial cell tube formation on gelled basement membrane extract. Nat Protoc. 2010; 5:628–635. http://dx.doi.org/10.1038/nprot.2010.6. [PubMed: 20224563]

Balaoing LR, Post AD, Liu H, Minn KT, Grande-Allen KJ. Age-related changes in aortic valve hemostatic protein regulation. Arterioscler Thromb Vasc Biol. 2014; 34:72–80. http://dx.doi.org/10.1161/ATVBAHA.113.301936. [PubMed: 24177329]

Benton JA, DeForest CA, Vivekanandan V, Anseth KS. Photocrosslinking of gelatin macromers to synthesize porous hydrogels that promote valvular interstitial cell function. Tissue Eng A. 2009; 15:3221–3230. http://dx.doi.org/10.1089/ten.TEA.2008.0545.

Bijman MNA, van Nieuw Amerongen GP, Laurens N, van Hinsbergh VWM, Boven E. Microtubule-targeting agents inhibit angiogenesis at subtoxic concentrations, a process associated with inhibition of Rac1 and Cdc42 activity and changes in the endothelial cytoskeleton. Mol Cancer Ther. 2006; 5:2348–2357. http://dx.doi.org/10.1158/1535-7163.MCT-06-0242. [PubMed: 16985069]

Bryan BA, Dennstedt E, Mitchell DC, Walshe TE, Noma K, Loureiro R, Saint-Geniez M, Campaigniac JP, Liao JK, D'Amore PA. RhoA/ROCK signaling is essential for multiple aspects of VEGF-mediated angiogenesis. FASEB J. 2010; 24:3186–3195. http://dx.doi.org/10.1096/fj.09-145102. [PubMed: 20400538]

Butcher JT, Nerem RM. Valvular endothelial cells regulate the phenotype of interstitial cells in co-culture: effects of steady shear stress. Tissue Eng. 2006; 12:905–915. http://dx.doi.org/10.1089/ten.2006.12.905. [PubMed: 16674302]

Butcher JT, Penrod AM, García AJ, Nerem RM. Unique morphology and focal adhesion development of valvular endothelial cells in static and fluid flow environments. Arterioscler Thromb Vasc Biol. 2004; 24:1429–1434. http://dx.doi.org/10.1161/01.ATV.0000130462.50769.5a. [PubMed: 15117733]

Butcher JT, Tressel S, Johnson T, Turner D, Sorescu G, Jo H, Nerem RM. Transcriptional profiles of valvular and vascular endothelial cells reveal phenotypic differences: influence of shear stress. Arterioscler Thromb Vasc Biol. 2006; 26:69–77. http://dx.doi.org/10.1161/01.ATV.0000196624.70507.0d. [PubMed: 16293796]

Butcher JT, Mahler GJ, Hockaday LA. Aortic valve disease and treatment: the need for naturally engineered solutions. Adv Drug Deliv Rev. 2011; 63:242–268. http://dx.doi.org/10.1016/j.addr.2011.01.008. [PubMed: 21281685]

Caira FC, Stock SR, Gleason TG, McGee EC, Huang J, Bonow RO, Spelsberg TC, McCarthy PM, Rahimtoola SH, Rajamannan NM. Human degenerative valve disease is associated with up-regulation of low-density lipoprotein receptor related protein 5 receptor-mediated bone formation. J Am Coll Cardiol. 2006; 47:1707–1712. http://dx.doi.org/10.1016/j.jacc.2006.02.040. [PubMed: 16631011]

Chalajour F, Treede H, Ebrahimnejad A, Lauke H, Reichenspurner H, Ergun S. Angiogenic activation of valvular endothelial cells in aortic valve stenosis. Exp Cell Res. 2004a; 298:455–464. http://dx.doi.org/10.1016/j.yexcr.2004.04.034. [PubMed: 15265693]

Chalajour F, Treede H, Ebrahimnejad A, Lauke H, Reichenspurner H, Ergun S. Angiogenic activation of valvular endothelial cells in aortic valve stenosis. Exp Cell Res. 2004b; 298:455–464. http://dx.doi.org/10.1016/j.yexcr.2004.04.034. [PubMed: 15265693]

Chalajour F, Treede H, Gehling UM, Ebrahimnejad A, Boehm DH, Riemer RK, Ergun S, Reichenspurner H. Identification and characterization of cells with high angiogenic potential and transitional phenotype in calcific aortic valve. Exp Cell Res. 2007; 313:2326–2335. http://dx.doi.org/10.1016/j.yexcr.2007.02.033. [PubMed: 17475245]

Charest, a; Pepin, A.; Shetty, R.; Côté, C. Distribution of SPARC during neovascularization of degenerative aortic stenosis. Heart. 2006; 92:1844–1849. http://dx.doi.org/10.1136/hrt.2005.086595. [PubMed: 16709694]

Chen MB, Srigunapalan S, Wheeler AR, Simmons CA. A 3D microfluidic platform incorporating methacrylated gelatin hydrogels to study physiological cardiovascular cell–cell interactions. Lab Chip. 2013; 13:2591–2598. http://dx.doi.org/10.1039/c3lc00051f. [PubMed: 23525275]

Cheung WY, Young EWK, Simmons CA. Techniques for isolating and purifying porcine aortic valve endothelial cells. J Heart Valve Dis. 2008; 17:674–681. [PubMed: 19137801]

Collett GDM, Canfield AE. Angiogenesis and pericytes in the initiation of ectopic calcification. Circ Res. 2005; 96:930–938. http://dx.doi.org/10.1161/01.RES.0000163634.51301.0d. [PubMed: 15890980]

Colomba A, Giuriato S, Dejean E, Thornber K, Delsol G, Tronchère H, Meggetto F, Payrastre B, Gaits-Iacovoni F. Inhibition of Rac controls NPM-ALK-dependent lymphoma development and dissemination. Blood Cancer J. 2011; 1:e21. http://dx.doi.org/10.1038/bcj.2011.19. [PubMed: 22829165]

Davis GE, Bayless KJ. An integrin and Rho GTPase-dependent pinocytic vacuole mechanism controls capillary lumen formation in collagen and fibrin matrices. Microcirculation. 2003; 10:27–44. http://dx.doi.org/10.1038/sj.mn.7800175. [PubMed: 12610662]

De Smet F, Segura I, De Bock K, Hohensinner PJ, Carmeliet P. Mechanisms of vessel branching: filopodia on endothelial tip cells lead the way. Arterioscler Thromb Vasc Biol. 2009; 29:639–649. http://dx.doi.org/10.1161/ATVBAHA.109.185165. [PubMed: 19265031]

Defilippi P, Olivo C, Venturino M, Dolce L, Silengo L, Tarone G. Actin cytoskeleton organization in response to integrin-mediated adhesion. Microsc Res Tech. 1999; 47:67–78. [PubMed: 10506763]

Duan B, Hockaday LA, Kang KH, Butcher JT. 3D bioprinting of heterogeneous aortic valve conduits with alginate/gelatin hydrogels. J Biomed Mater Res A. 2013a; 101:1255–1264. http://dx.doi.org/10.1002/jbm.a.34420. [PubMed: 23015540]

Duan B, Hockaday LA, Kapetanovic E, Kang KH, Butcher JT. Stiffness and adhesivity control aortic valve interstitial cell behavior within hyaluronic acid based hydrogels. Acta Biomater. 2013b; 9:7640–7650. http://dx.doi.org/10.1016/j.actbio.2013.04.050. [PubMed: 23648571]

Duran CM, Gunning AJ. The vascularization of the heart valves: a comparative study. Cardiovasc Res. 1968; 2:290–296. [PubMed: 5670736]

Durst CA, Cuchiara MP, Mansfield EG, West JL, Grande-Allen KJ. Flexural characterization of cell encapsulated PEGDA hydrogels with applications for tissue engineered heart valves. Acta Biomater. 2011; 7:2467–2476. http://dx.doi.org/10.1016/j.actbio.2011.02.018. [PubMed: 21329770]

Eming SA, Hubbell JA. Extracellular matrix in angiogenesis: dynamic structures with translational potential. Exp Dermatol. 2011; 20:605–613. http://dx.doi.org/10.1111/j.1600-0625.2011.01309.x. [PubMed: 21692861]

Eslami, M.; Vrana, NE.; Zorlutuna, P.; Sant, S.; Jung, S.; Masoumi, N.; Khavari-Nejad, RA.; Javadi, G.; Khademhosseini, A. Fiber-reinforced hydrogel scaffolds for heart valve tissue engineering. J Biomater Appl. 2014. http://dx.doi.org/10.1177/0885328214530589

Go AS, Mozaffarian D, Roger VL, Benjamin EJ, Berry JD, Blaha MJ, Dai S, Ford ES, Fox CS, Franco S, Fullerton HJ, Gillespie C, Hailpern SM, Heit JA, Howard VJ, Huffman MD, Judd SE, Kissela BM, Kittner SJ, Lackland DT, Lichtman JH, Lisabeth LD, Mackey RH, Magid DJ, Marcus GM, Marelli A, Matchar DB, McGuire DK, Mohler ER, Moy CS, Mussolino ME, Neumar RW, Nichol G, Pandey DK, Paynter NP, Reeves MJ, Sorlie PD, Stein J, Towfighi A, Turan TN, Virani SS, Wong ND, Woo D, Turner MB. Heart disease and stroke statistics—2014 update: a report from the American Heart Association. Circulation. 2014; 129:e28–e292. http://dx.doi.org/10.1161/01.cir.0000441139.02102.80. [PubMed: 24352519]

Gould, ST.; Anseth, KS. Role of cell–matrix interactions on VIC phenotype and tissue deposition in 3D PEG hydrogels. J Tissue Eng Regen Med. 2013. http://dx.doi.org/10.1002/term.1836

Gould DJ, Vadakkan TJ, Poché RA, Dickinson ME. Multifractal and lacunarity analysis of microvascular morphology and remodeling. Microcirculation. 2011; 18:136–151. http://dx.doi.org/10.1161/ATVBAHA.111.227868.Vascular. [PubMed: 21166933]

Gould ST, Matherly EE, Smith JN, Heistad DD, Anseth KS. The role of valvular endothelial cell paracrine signaling and matrix elasticity on valvular interstitial cell activation. Biomaterials. 2014; 35:3596–3606. http://dx.doi.org/10.1016/j.biomaterials.2014.01.005. [PubMed: 24462357]

Gu X, Masters KS. Role of the Rho pathway in regulating valvular interstitial cell phenotype and nodule formation. Am J Physiol Heart Circ Physiol. 2011; 300:H448–H458. http://dx.doi.org/10.1152/ajpheart.01178.2009. [PubMed: 21131478]

Hakuno, D.; Kimura, N.; Yoshioka, M. Periostin advances atherosclerotic and rheumatic cardiac valve degeneration by inducing angiogenesis and MMP production in humans and rodents; J Clin Invest. 2010. p. 120http://dx.doi.org/10.1172/JCI40973DS1

He KL, Deora AB, Xiong H, Ling Q, Weksler BB, Niesvizky R, Hajjar KA. Endothelial cell annexin A2 regulates polyubiquitination and degradation of its binding partner S100A10/p11. J Biol Chem. 2008; 283:19192–19200. http://dx.doi.org/10.1074/jbc.M800100200. [PubMed: 18434302]

Hinton RB, Yutzey KE. Heart valve structure and function in development and disease. Annu Rev Physiol. 2011; 73:29–46. http://dx.doi.org/10.1146/annurev-physiol-012110-142145. [PubMed: 20809794]

Hoang MV, Whelan MC, Senger DR. Rho activity critically and selectively regulates endothelial cell organization during angiogenesis. Proc Natl Acad Sci US A. 2004; 101:1874–1879. http://dx.doi.org/10.1073/pnas.0308525100.

Holmes K, Roberts OL, Thomas AM, Cross MJ. Vascular endothelial growth factor receptor-2: structure, function, intracellular signalling and therapeutic inhibition. Cell Signal. 2007; 19:2003–2012. http://dx.doi.org/10.1016/j.cellsig.2007.05.013. [PubMed: 17658244]

Huber AB, Kolodkin AL, Ginty DD, Cloutier JF. Signaling at the growth cone: ligand–receptor complexes and the control of axon growth and guidance. Annu Rev Neurosci. 2003; 26:509–563. http://dx.doi.org/10.1146/annurev.neuro.26.010302.081139. [PubMed: 12677003]

Ishijima M, Suzuki N, Hozumi K, Matsunobu T, Kosaki K, Kaneko H, Hassell JR, Arikawa-Hirasawa E, Yamada Y. Perlecan modulates VEGF signaling and is essential for vascularization in endochondral bone formation. Matrix Biol. 2012; 31:234–245. http://dx.doi.org/10.1016/j.matbio.2012.02.006. [PubMed: 22421594]

Ishizaki T, Uehata M, Tamechika I, Keel J, Nonomura K, Maekawa M, Narumiya S. Pharmacological properties of Y-27632, a specific inhibitor of Rho-associated kinases. Mol Pharmacol. 2000; 57:976–983. [PubMed: 10779382]

Jian B, Narula N, Li Q, Mohler ER, Levy RJ. Progression of aortic valve stenosis: TGF-beta1 is present in calcified aortic valve cusps and promotes aortic valve interstitial cell calcification via apoptosis. Ann Thorac Surg. 2003; 75:457–465. discussion 465–6. [PubMed: 12607654]

Kalluri R. Basement membranes: structure, assembly and role in tumour angiogenesis. Nat Rev Cancer. 2003; 3:422–433. http://dx.doi.org/10.1038/nrc1094. [PubMed: 12778132]

Kirschner, CM.; Alge, DL.; Gould, ST.; Anseth, KS. Clickable, photodegradable hydrogels to dynamically modulate valvular interstitial cell phenotype. Adv Health Mater. 2014. http://dx.doi.org/10.1002/adhm.201300288

Lamalice L, Le Boeuf F, Huot J. Endothelial cell migration during angiogenesis. Circ Res. 2007; 100:782–794. http://dx.doi.org/10.1161/01.RES.0000259593.07661.1e. [PubMed: 17395884]

Lee SH, Kunz J, Lin SH, Yu-Lee L. 16-kDa prolactin inhibits endothelial cell migration by down-regulating the Ras-Tiam1-Rac1-Pak1 signaling pathway. Cancer Res. 2007; 67:11045–11053. http://dx.doi.org/10.1158/0008-5472.CAN-07-0986. [PubMed: 18006851]

Mariscalco G, Lorusso R, Sessa F, Bruno VD, Piffaretti G, Banach M, Cattaneo P, Cozzi GP, Sala A. Imbalance between pro-angiogenic and anti-angiogenic factors in rheumatic and mixomatous mitral valves. Int J Cardiol. 2011; 152:337–344. http://dx.doi.org/10.1016/j.ijcard.2010.08.001. [PubMed: 20832876]

Mazzone A, Epistolato MC, De Caterina R, Storti S, Vittorini S, Sbrana S, Gianetti J, Bevilacqua S, Glauber M, Biagini A, Tanganelli P. Neoangiogenesis, T-lymphocyte infiltration, and heat shock protein-60 are biological hallmarks of an immunomediated inflammatory process in end-stage calcified aortic valve stenosis. J Am Coll Cardiol. 2004; 43:1670–1676. http://dx.doi.org/10.1016/j.jacc.2003.12.041. [PubMed: 15120829]

Mohler ER, Chawla MK, Chang AW, Vyavahare N, Levy RJ, Graham L, Gannon FH. Identification and characterization of calcifying valve cells from human and canine aortic valves. J Heart Valve Dis. 1999; 8:254–260. [PubMed: 10399657]

Mohler ER III, Gannon FH, Reynolds C, Zimmerman R, Keane MG, Kaplan FS. Bone formation and inflammation in cardiac valves. Circulation. 2001; 103:1522–1528. [PubMed: 11257079]

Nakajima Y, Mironov V, Yamagishi T, Nakamura H, Markwald RR. Expression of smooth muscle alpha-actin in mesenchymal cells during formation of avian endocardial cushion tissue: a role for transforming growth factor beta3. Dev Dyn. 1997; 209:296–309. http://dx.doi.org/10.1002/(SICI)1097-0177(199707)209:3b296::AIDAJA5N3.0.CO;2-D. [PubMed: 9215644]

O'Brien KD, Kuusisto J, Reichenbach DD, Ferguson M, Giachelli CM, Alpers CE, Otto CM. Osteopontin is expressed in human aortic valvular lesions. Circulation. 1995; 92:2163–2168. http://dx.doi.org/10.1161/01.CIR.92.8.2163. [PubMed: 7554197]

Paranya G, Vineberg S, Dvorin E, Kaushal S, Roth SJ, Rabkin E, Schoen FJ, Bischoff J. Aortic valve endothelial cells undergo transforming growth factor-beta-mediated and non-transforming growth factor-beta-mediated transdifferentiation in vitro. Am J Pathol. 2001; 159:1335–1343. [PubMed: 11583961]

Poggio P, Grau JB, Field BC, Sainger R, Seefried WF, Rizzolio F, Ferrari G. Osteopontin controls endothelial cell migration in vitro and in excised human valvular tissue from patients with calcific aortic stenosis and controls. J Cell Physiol. 2011; 226:2139–2149. http://dx.doi.org/10.1002/jcp.22549. [PubMed: 21520066]

Pollard TD, Borisy GG. Cellular motility driven by assembly and disassembly of actin filaments. Cell. 2003; 112:453–465. [PubMed: 12600310]

Rajamannan NM, Nealis TB, Subramaniam M, Pandya S, Stock SR, Ignatiev CI, Sebo TJ, Rosengart TK, Edwards WD, McCarthy PM, Bonow RO, Spelsberg TC. Calcified rheumatic valve neoangiogenesis is associated with vascular endothelial growth factor expression and osteoblast-like bone formation. Circulation. 2005; 111:3296–3301. http://dx.doi.org/10.1161/CIRCULATIONAHA.104.473165. [PubMed: 15956138]

Rodriguez L, Wu X, Guan J. Wound-healing assay. Cell Migr. 2005; 294:23–29. http://dx.doi.org/10.1385/1-59259-860-9:023.

Sakabe M, Ikeda K, Nakatani K, Kawada N, Imanaka-Yoshida K, Yoshida T, Yamagishi T, Nakajima Y. Rho kinases regulate endothelial invasion and migration during valvuloseptal endocardial cushion tissue formation. Dev Dyn. 2006; 235:94–104. http://dx.doi.org/10.1002/dvdy.20648. [PubMed: 16342113]

Soini Y, Salo T, Satta J. Angiogenesis is involved in the pathogenesis of nonrheumatic aortic valve stenosis. Hum Pathol. 2003; 34:756–763. http://dx.doi.org/10.1016/S0046-8177(03)00245-4. [PubMed: 14506635]

Stephens EH, Durst CA, West JL, Grande-Allen KJ. Mitral valvular interstitial cell responses to substrate stiffness depend on age and anatomic region. Acta Biomater. 2011; 7:75–82. http://dx.doi.org/10.1016/j.actbio.2010.07.001. [PubMed: 20624493]

Syväranta S, Helske S, Laine M, Lappalainen J, Kupari M, Mäyränpää MI, Lindstedt Ka, Kovanen PT. Vascular endothelial growth factor-secreting mast cells and myofibroblasts: a novel self-perpetuating angiogenic pathway in aortic valve stenosis. Arterioscler Thromb Vasc Biol. 2010; 30:1220–1227. http://dx.doi.org/10.1161/ATVBAHA.109.198267. [PubMed: 20299690]

Takada Y, Khuri FR, Aggarwal BB. Protein farnesyltransferase inhibitor (SCH 66336) abolishes NF-kappaB activation induced by various carcinogens and inflammatory stimuli leading to suppression of NF-kappaB-regulated gene expression and up-regulation of apoptosis. J Biol Chem. 2004; 279:26287–26299. http://dx.doi.org/10.1074/jbc.M400963200. [PubMed: 15090542]

Tao G, Kotick JD, Lincoln J. Heart valve development, maintenance, and disease: the role of endothelial cells. Curr Top Dev Biol. 2012; 100:203–232. http://dx.doi.org/10.1016/B978-0-12-387786-4.00006-3. [PubMed: 22449845]

Teo KK, Corsi DJ, Tam JW, Dumesnil JG, Chan KL. Lipid lowering on progression of mild to moderate aortic stenosis: meta-analysis of the randomized placebocontrolled clinical trials on 2344 patients. Can J Cardiol. 2011; 27:800–808. http://dx.doi.org/10.1016/j.cjca.2011.03.012. [PubMed: 21742465]

Tseng H, Balaoing LR, Grigoryan B, Raphael RM, Killian TC, Souza GR, GrandeAllen KJ. A three-dimensional co-culture model of the aortic valve using magnetic levitation. Acta Biomater. 2014; 10:173–182. http://dx.doi.org/10.1016/j.actbio.2013.09.003. [PubMed: 24036238]

Wang H, Sridhar B, Leinwand LA, Anseth KS. Characterization of cell subpopulations expressing progenitor cell markers in porcine cardiac valves. PLoS One. 2013; 8:e69667. http://dx.doi.org/10.1371/journal.pone.0069667. [PubMed: 23936071]

Weind KL, Ellis CG, Boughner DR. Aortic valve cusp vessel density: relationship with tissue thickness. J Thorac Cardiovasc Surg. 2002; 123:333–340. http://dx.doi.org/10.1067/mtc.2002.119696. [PubMed: 11828294]

Xu S, Liu S, Eastwood M, Sonnylal S, Denton CP, Abraham DJ, Leask A. Rac inhibition reverses the phenotype of fibrotic fibroblasts. PLoS One. 2009; 4:e7438. http://dx.doi.org/10.1371/journal.pone.0007438. [PubMed: 19823586]

Xu S, Liu AC, Gotlieb AI. Common pathogenic features of atherosclerosis and calcific aortic stenosis: role of transforming growth factor-beta. Cardiovasc Pathol. 2010; 19:236–247. http://dx.doi.org/10.1016/j.carpath.2009.09.007. [PubMed: 19942455]

Yang JH, Wylie-Sears J, Bischoff J. Opposing actions of Notch1 and VEGF in postnatal cardiac valve endothelial cells. Biochem Biophys Res Commun. 2008; 374:512–516. http://dx.doi.org/10.1016/j.bbrc.2008.07.057. [PubMed: 18647596]

Yin L, Morishige KI, Takahashi T, Hashimoto K, Ogata S, Tsutsumi S, Takata K, Ohta T, Kawagoe J, Takahashi K, Kurachi H. Fasudil inhibits vascular endothelial growth factor-induced angiogenesis in vitro and in vivo. Mol Cancer Ther. 2007; 6:1517–1525. http://dx.doi.org/10.1158/1535-7163.MCT-06-0689. [PubMed: 17513600]

Yoshioka M, Yuasa S, Matsumura K, Kimura K, Shiomi T, Kimura N, Shukunami C, Okada Y, Mukai M, Shin H, Yozu R, Sata M, Ogawa S, Hiraki Y, Fukuda K. Chondromodulin-I maintains cardiac valvular function by preventing angiogenesis. Nat Med. 2006; 12:1151–1159. http://dx.doi.org/10.1038/nm1476. [PubMed: 16980969]

Zudaire E, Gambardella L, Kurcz C, Vermeren S. A computational tool for quantitative analysis of vascular networks. PLoS One. 2011; 6:e27385. http://dx.doi.org/10.1371/journal.pone.0027385. [PubMed: 22110636]

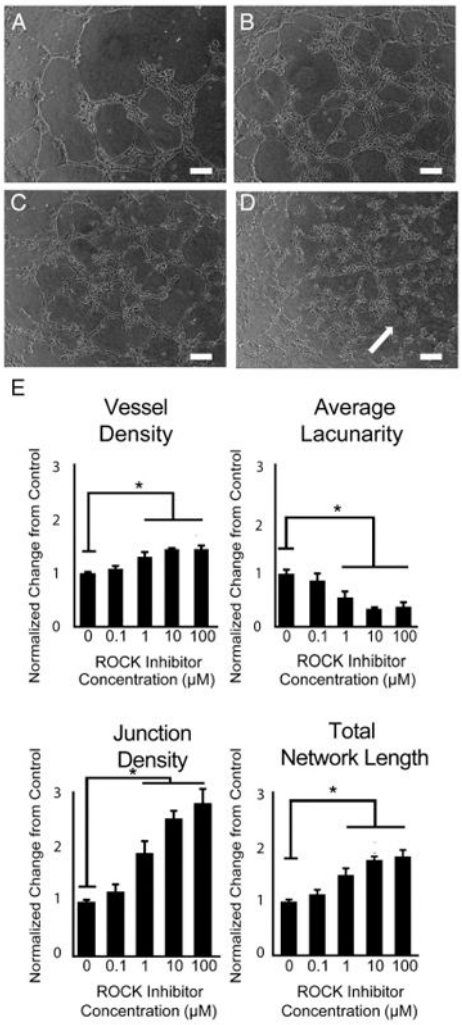

Fig. 1.

ROCK inhibition increases APAVEC network complexity in vitro. Representative images of the networks formed by APAVECs treated with A) PBS, B) 1 μM, C) 10 μM, D) 100 μM of the ROCK inhibitor. APAVECs form more complex networks and have increased lamellipodia (white arrow) with higher concentrations of the ROCK inhibitor. Scale bars represent 100 μm. E) Quantification of dose dependent changes in various network metrics. Results are shown as mean ± standard error normalized to the control ($n = 9$, ANOVA $p < 0.0001$ for all but average lacunarity for which p-value < 0.005. *$p < 0.05$ vs. control, Tukey's HSD).

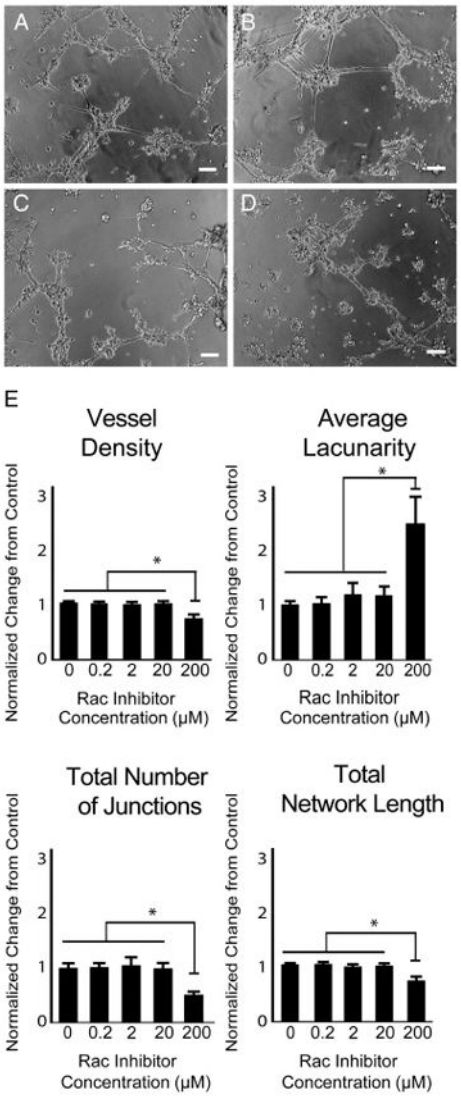

Fig. 2.

Rac inhibition decreases APAVEC network complexity in vitro. Representative images of APAVEC network formation based upon treatment with A) PBS, B) 2 μM, C) 20 μM, or D) 200 μM of the Rac inhibitor. APAVEC form smaller and less dense networks at the highest treatments with the Rac inhibitor. Scale bars represent 100 μm. E) Quantification of the changes in various network metrics. Results are shown as mean ± standard error normalized to the control ($n = 9$, $^*p < 0.05$ vs. all other groups, Tukey's HSD). Although there were trends in some of the measured network metrics, the lower concentrations of Rac inhibitor resulted in less pronounced effects that did not attain statistical significance.

Health Research Alliance Author Manuscript

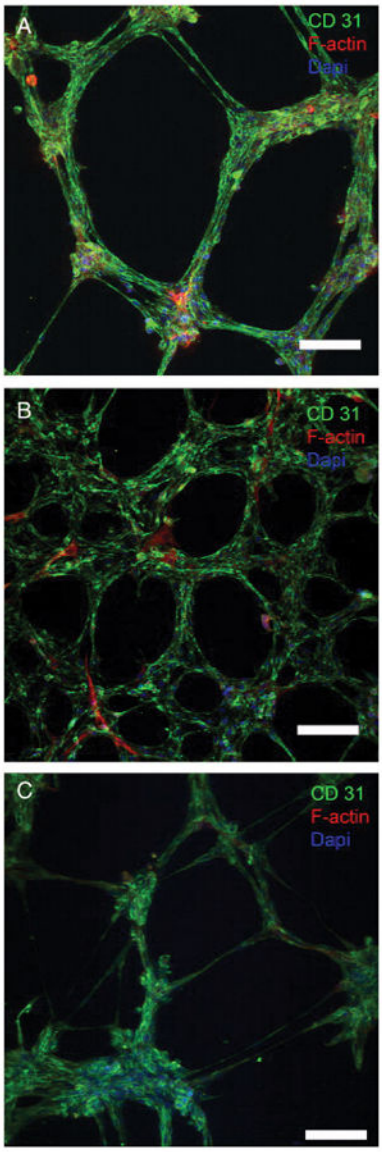

Fig. 3.

Representative Z-stack reconstructed confocal fluorescence microscopy images of APAVEC networks treated with A) PBS, B) 50 μM of ROCK inhibitor, or C) 100 μM of Rac inhibitor taken with a 10 × objective. Control APAVECs organized into tightly bound complex linear tubule-like networks, but the ROCK inhibited APAVECs formed flat networks with looser organization and ablated tubule formation. Compared to the control, Rac1 inhibition appeared to affect the initiation of the tubule formation shown by their fewer tubule like structure numbers between nodes. However, tube-like structures that did form demonstrated tightly clustered cell assemblies and aligned actin structures, similar to the control tubule like structures. Green: CD31. Red: aSMA. Blue: DAPI. Scale bars represent 100 μm.

Health Research Alliance Author Manuscript

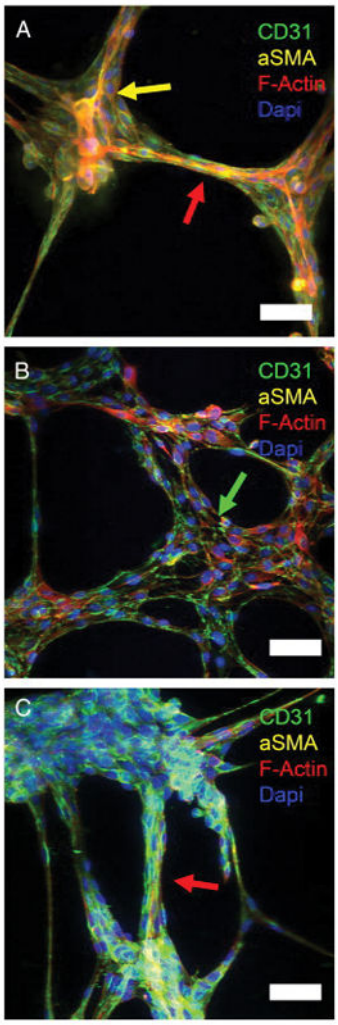

Fig. 4.

Z-stack reconstructed confocal microscopy images of APAVEC networks treated with A) PBS, B) 50 μM of ROCK inhibitor, C) or 100 μM of Rac inhibitor. Images were taken with a 20 × objective. Aligned actin structures and close cell–cell organization typical of tubule-like sprouts (red arrow) were found in the (A) control and (C) Rac-inhibited networks, but neither of these features were displayed in the (B) ROCK-inhibited networks (green arrow). In each case, a few aSMA+/CD31− cells were found binding several CD31+ VECs (yellow arrow). Scale bars represent 50 μm. Green: CD31. Yellow: aSMA. Red: F-actin. Blue: DAPI.

Health Research Alliance Author Manuscript

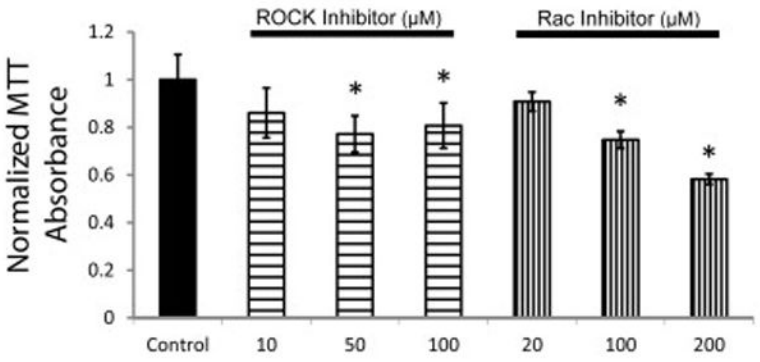

Fig. 5.

Quantification of changes in cell number based upon ROCK or Rac1 inhibition. Results are displayed as the mean absorbance relative to the control at 24 h ± standard deviation (n = 6, *$p < 0.05$ vs. control).

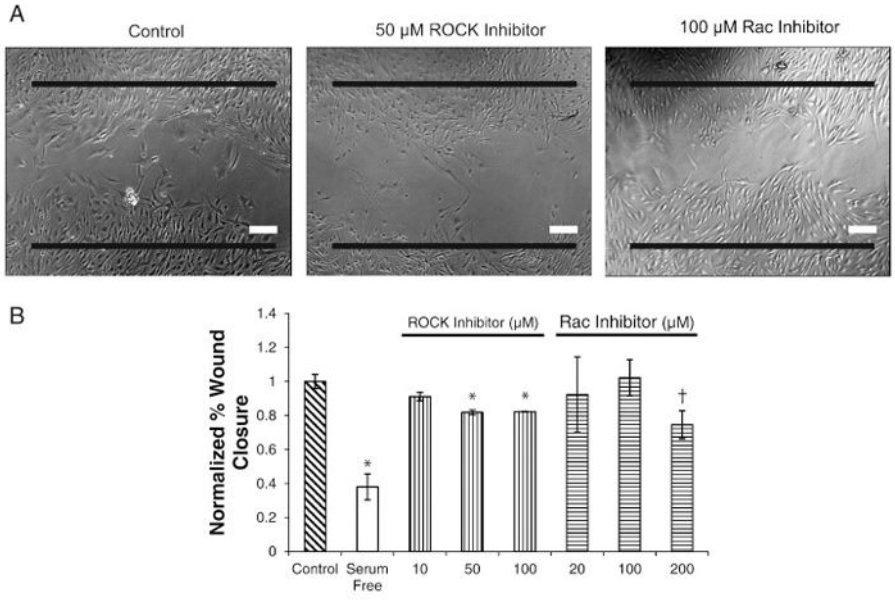

Fig. 6.

ROCK and Rac regulated APAVEC migration in a scratch wound healing assay. A) Representative images of APAVEC wounds 24 h after injury when treated with 50 μM ROCK inhibitor or 100 μM Rac inhibitor. The black lines represent the size of the initial wound. Scale bar represents 100 μm. B) Quantification of wound closure at 24 h. Results are displayed as the mean percent wound closure normalized to the control ± standard error. (n = 4–6, *$p < 0.05$ vs. control; †$p = 0.08$ vs. control.)

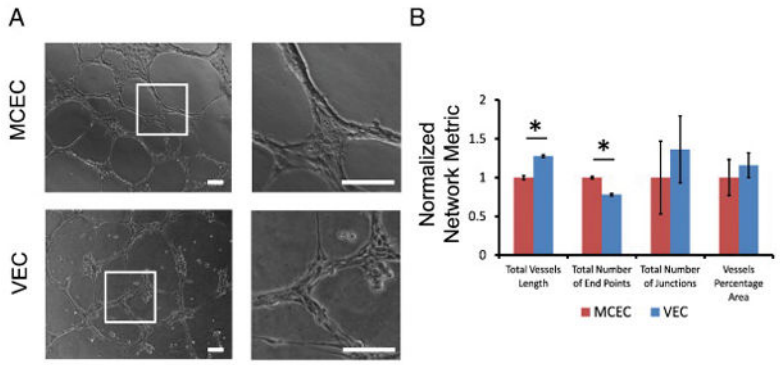

Fig. 7.

APAVEC network formation was directly compared to MCEC network formation to elucidate differences in their angiogenic signal transduction. A) At 7 h, both VECs and MCECs displayed branching complex networks, but MCECs displayed smoother tubule formation as individual cells were more difficult to discern. Scale bars represent 50 μm. B) Quantification of the VEC networks relative to the MCEC networks demonstrated a larger total network size and lower number of end points for VEC-generated networks ($n = 15$, $^*p < 0.05$ between cell types). The networks demonstrated no significant difference in lacunarity or junction density, but there was a trend of the VECs having a larger total number of junctions and total vessel percentage area ($p = 0.07$ and 0.06 respectively). Data is displayed as average ± standard deviation normalized to the MCEC metrics.

Health Research Alliance Author Manuscript

Table 1

Characteristics of tubule-like networks formed by APAVECs under control conditions.

Vascular Network Metric	Value
Vessel density (%)	45 ± 1.6
Junction density (%)	36 ± 2
Total number of junctions	38 ± 2.3
Total number of end points	25 ± 1.4
Total vessel length (mm)	8.2 ± 0.38
Lacunarity	0.22 ± 0.02

Values are reported as the average ± the standard error (n = 14).